Photoreceptive net in the mammalian retina

This mesh of cells may explain how some blind mice can still tell day from night.

We have discovered an expansive photoreceptive 'net' in the mouse inner retina, visualized by using an antiserum against melanopsin, a likely photopigment[1,2]. This immunoreactivity is evident in a subset of retinal ganglion cells that morphologically resemble those that project to the suprachiasmatic nucleus (SCN), the site of the primary circadian pacemaker[3,4]. Our results indicate that this bilayered photoreceptive net is anatomically distinct from the rod and cone photoreceptors of the outer retina, and suggest that it may mediate non-visual photoreceptive tasks such as the regulation of circadian rhythms.

Most SCN-projecting retinal ganglion cells express melanopsin messenger RNA[5]. SCN-projecting retinal gangion cells are also photosensitive[6] and have spectral absorbance profiles that are characteristic of opsin-based photopigments[6]. The dimensions of the receptive fields of these cells are identical to those of their dendritic fields, indicating that photopigments that are capable of activating the depolarizing responses may reside in the dendrites (D. M. Berson *et al.*, personal communication).

We have found that melanopsin, the only opsin known to exist in retinal ganglion cells, is indeed expressed in the dendrites of this small subset of retinal ganglion cells (Fig. 1). Most striking are the plexuses formed by immunopositive dendrites in the outermost and innermost laminae of the inner plexiform layer (Fig. 2). These cells form an extensive network of opsin-containing dendrites, a photoreceptive apparatus previously overlooked in the mammalian retina.

The mammalian eye must complete two distinct photoreceptive tasks: vision and irradiance detection. Vision requires a fine array of 'narrow-capture' photoreceptive elements that allows fine spatial resolution; the photoreceptors (rods and cones) and downstream inner-retinal neurons involved in vision have been well characterized. By contrast, tasks such as photic regulation of circadian rhythms require the detection of changes in ambient irradiance, for which fine spatial resolution is not only unnecessary but may even confound the system. The retinal structures required for this 'broad-capture' photoreception have so far not been identified.

One strategy to determine irradiance levels from large sectors of visual space is to sum or average the outputs of many narrow-capture photoreceptors. Alternatively, a distinct anatomical apparatus may fulfil the requirement for a broad-capture, integrating photoreceptive system. The expansive photoreceptive net described here within the inner retina could serve such a function. Moreover, this photoreceptive system could explain why photo-entrainment of circadian rhythms is abolished by bilateral eye removal, yet persists in mice that lack rods and cones[7].

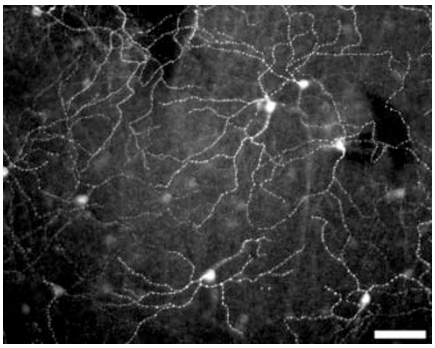

Figure 1 The photoreceptive net in the mouse inner retina. Immunofluorescent labelling of melanopsin-containing retinal ganglion cells on a flat mount of mouse retina reveals an extensive network of immunopositive dendrites. Scale bar, 100 μm.

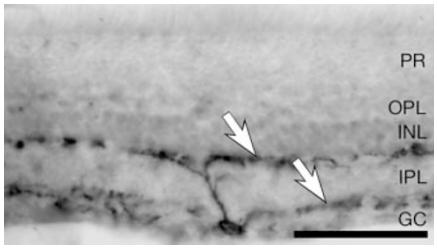

Figure 2 Cross-section of a mouse retina, with a single melanopsin-positive retinal ganglion cell. Note the two plexuses (arrows) of immunoreactive dendrites. GC, ganglion cells; IPL, inner plexiform layer; INL, inner nuclear layer; OPL, outer plexiform layer; PR, photoreceptors. Scale bar, 100 μm.

Ignacio Provencio, Mark D. Rollag, Ana Maria Castrucci
Department of Anatomy, Physiology and Genetics, and the Circadian Research Center, Uniformed Services University, Bethesda, Maryland 20814, USA
e-mail: iprovencio@usuhs.mil

1. Provencio, I. *et al. J. Neurosci.* **20,** 600–605 (2000).
2. Rollag, M. D., Provencio, I., Sugden, D. & Green, C. B. *Methods Enzymol.* **316,** 291–309 (2000).
3. Provencio, I., Cooper, H. M. & Foster, R. G. *J. Comp. Neurol.* **395,** 417–439 (1998).
4. Moore, R. Y., Speh, J. C. & Card, J. P. *J. Comp. Neurol.* **352,** 351–366 (1995).
5. Gooley, J. J., Lu, J., Chou, T. C., Scammell, T. E. & Saper, C. B. *Nature Neurosci.* **4,** 1165 (2001).
6. Berson, D. M., Dunn, F. A. & Takao, M. *Invest. Ophthalmol. Vis. Sci.* **42,** S113 Abstr. 613 (2001).
7. Freedman, M. S. *et al. Science* **284,** 502–504 (1999).

Competing financial interests: declared none.

Satellite imaging

Massive emissions of toxic gas in the Atlantic

Recurrent eruptions of toxic hydrogen sulphide gas in the waters along the Namibian coast off southwestern Africa have been considered to be local features with only limited ecosystem-scale consequences. But satellite remote sensing has revealed that these naturally occurring events are much more extensive and longer-lasting than previously suspected, and that the resultant hypoxia may last for much longer. The effects on the marine ecology and valuable coastal fisheries of this region are likely to be important.

In this richly productive coastal oceanic region[1–3], areas of seafloor hypoxia (<0.5 ml O_2 l^{-1}), and even total anoxia, are extensive, and it is beneath these that toxic hydrogen sulphide can be generated within a metres-deep layer of diatom ooze. People living along the coast have become inured to the disagreeable smells and corrosive effects of sulphurous gases released from the sea, which kill a variety of nearshore fish and invertebrates annually. This results in a fortuitous feast for seabirds, which converge on the milky turquoise-coloured patches of sulphide-infused waters to feed on floating casualties, and also for the local people, who eagerly harvest rock lobsters fleeing ashore from the noxious conditions in the water. However, the sheer magnitude of the extent, frequency and duration of these phenomena, as revealed by our recent satellite observations, was not realized.

For example, a quasi-true-colour image from the OrbView-2 SeaWIFS satellite for 18 March 2001 (Fig. 1a) shows an extended turquoise patch stretching more than 200 km along the Namib Desert coast. Ground personnel simultaneously recorded the hydrogen sulphide in water samples, together with observations of noxious sulphide odours, seabirds feeding on floating dead marine organisms, sharply anomalous dislocation of lobster distributions towards the shore, and so on, constituting evidence of intense hydrogen sulphide emissions in that zone. The concentration of dissolved oxygen was very low even in the surface 'milky' water (0.7 ml l^{-1}); the milky discoloration is created by the slurry of highly

© 2002 Macmillan Magazines Ltd

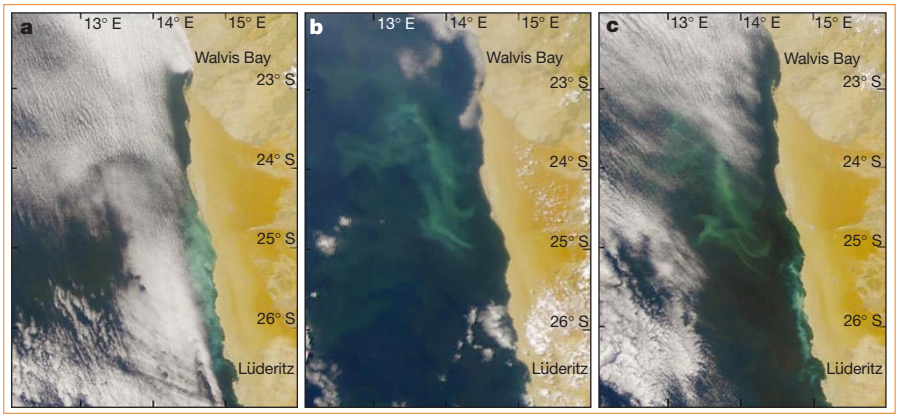

Figure 1 Sea-surface distribution of suspended sulphur granules. Quasi-true-colour images for the region at latitude 12° E–16° E, longitude 22° S–27° S, off south-central Namibia; images were generated from the OrbView-2 SeaWiFS satellite during March–April 2001. The milky turquoise coloration represents high concentrations of suspended sulphur granules. Data were collected on **a,** 18 March; **b,** 29 March; and **c,** 3 April 2001.

reflective precipitated microgranules of sulphur resulting from the oxidation of sulphide ions near the oxygenated sea surface.

In the days that followed, the feature was observed from satellite pictures to be advected northwards and offshore in the prevailing equatorward geostrophic current flow and offshore-directed surface-wind drift fields, which are characteristic of such eastern-ocean coastal upwelling systems[4], to reach the position and configuration seen in Fig. 1b. In the image of 3 April (Fig. 1c), even while the earlier offshore feature continues to maintain a coherent identity, another totally new hydrogen sulphide emission event is seen to have started abruptly within the coastal upwelling zone north of Lüderitz.

Once the earlier feature had separated from the coast, it took on an appearance superficially similar to that in satellite views of very large coccolithophore blooms[5]. However, the continuity of the feature in the available satellite views and the advective context, as inferred from the evolution of satellite-sensed ocean surface temperature, make it clear that the offshore feature is the same as that previously observed as an intense episode of sulphide emission nearer the coast. The zone of intense coloration in later images (Fig. 1b) extends over an expanse of total sea surface greater than 20,000 km^2.

Such episodes have been recorded somewhere along the coast of Namibia more often than not during the recent months since the satellite observational capability was recognized. Where verification on the ground has been available, the early stages of these events have likewise been confirmed to be associated with sulphide emissions. In addition to its directly toxic effects, hydrogen sulphide strips dissolved oxygen from the water column, leaving behind a subsurface hypoxia that is manifested visibly as the sulphur-infused sea surface. It is this subsurface hypoxia, which might endure well beyond the period when the toxic sulphide gas is present, that could pose the principal ecological problem. An event, first clearly noted on 17 May 2001, was still plainly visible as late as 6 June 2001.

Scarla J. Weeks*, Bronwen Currie†, Andrew Bakun‡

**Ocean Space Ltd, and ‡IRD, IDYLE Project, Oceanography Department, University of Cape Town, Rondebosch 7701, South Africa*
e-mail: oceanspace@icon.co.za
†National Marine Research and Information Center, Swakopmund, Namibia

1. Bailey, G. W., Beyers, C. J. deB. & Lipschitz, S. R. *S. Afr. J. Mar. Sci.* **3,** 197–214 (1985).
2. Mas-Riera, J., Lombarte, A., Gordoa, A. & Macpherson, E. *Marine Biol.* **104,** 175–182 (1990).
3. Hamukuaya, H., O'Toole, M. J. & Woodhead, P. M. J. *S. Afr. J. Mar. Sci.* **19,** 57–59 (1998).
4. Wooster, W. S. & Reid, J. L. in *The Sea* Vol. 2 (ed. Hill, M. N.) 253–280 (Interscience, New York, 1963).
5. Tyrrell, T., Holligan, P. M. & Mobley, C. D. *J. Geophys. Res.* **104,** 3223–3241 (1999).

Competing financial interests: declared none.

Biomechanics

Dinosaur locomotion from a new trackway

Ardley Quarry in Oxfordshire, UK, contains one of the most extensive dinosaur-trackway sites in the world, with individual trackways extending for up to 180 metres. We have discovered a unique dual-gauge trackway from a bipedal theropod dinosaur from the Middle Jurassic in this locality, which indicates that these large theropods were able to run and that they used different hindlimb postures for walking and running. Our findings have implications for the biomechanics and evolution of theropod locomotion.

The Ardley trackways are preserved on a single horizon of the Middle Bathonian (163 million years old)[1] white-limestone formation and include those from large theropods and at least two types of sauropod dinosaur. Three of the trackways (numbered 13, 29 and 80; J.J.D., unpublished observations) comprise large tridactyl ('three-toed') prints, with narrow claw impressions typical of theropod dinosaurs (Fig. 1). All three trackways (except for a section of track 13) are wide-gauge, with the prints indicating that the hind feet were placed sequentially in a zig-zag arrangement separated widely from the midline (Fig. 1a). Stride length (2.70 m) and pace angulation (117°–132°; Fig. 1) remain constant throughout the wide-gauge tracks. This pattern contrasts strongly with the more usual narrow-gauge form of theropod trackway[2,3] in which pace-angulation values range between 160° and 170°: the hind-foot impressions are located close to the midline of the trackway.

Trackway 13 is unique because one section shows the theropod gait switching from wide to narrow gauge (the stride length increases to 5.65 m and pace angulation increases to 173°; Fig. 2). The orientation of the feet also changes from positive rotation (toes directed forwards and inwards; Fig. 1a) during wide-gauge locomotion, to a small negative rotation (toes directed slightly outwards) during the narrow-gauge phase (Fig. 1b).

Estimating the speed of movement of the track-maker requires information on

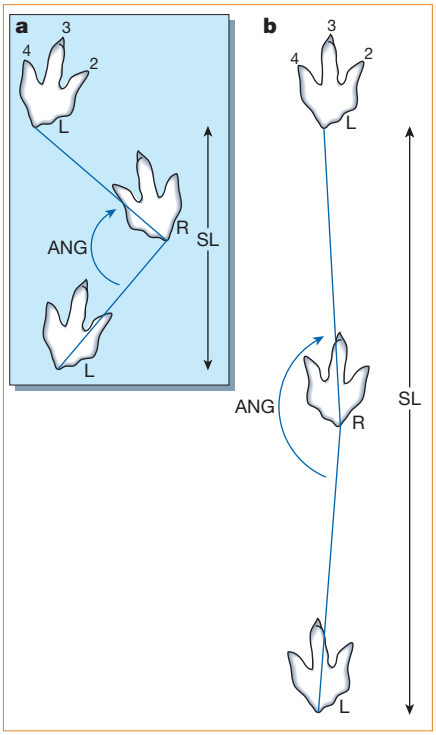

Figure 1 The dual-gait features of theropod trackway 13 from Ardley Quarry, Oxfordshire, UK. **a,** Wide-gauge section; **b,** narrow-gauge section. Digits are numbered and footprints are identified as left (L) and right (R); ANG, pace angulation; SL, stride length.

© 2002 Macmillan Magazines Ltd